where $\mathbf{r}_d$ and $\mathbf{R}$ refer to the coordinates of the outgoing and captured deuterons. Assuming the Gaussian form for the internal wave function of the α particle and using the relation (13) above, one may write $\varphi(r_\alpha) = c\exp[-4\gamma^2\rho^2]$, where the binding energy constant γ may have now a different value from that considered above. c is a constant factor. Following the same method used in Sec. I above, one gets for the (α,d) differential cross section

$$d\sigma \cong \exp[-K^2/8\gamma^2] \sum_L A_L^2 F_L^2(QR_0)/Q^2R_0^2.$$

This has the same form as Eq. (16) above.

Carrying out the same calculation for the (α,p) and using the following form for the internal wave function $\varphi(r_\alpha) = c\exp[-3\gamma^2\rho^2]$, see Fig. 1(c), one gets for the differential cross section the value

$$d\sigma \cong \exp[-K^2/6\gamma^2] \sum_L A_L^2 F_L^2(QR_0)/Q^2R_0^2, \quad \text{(A19)}$$

which is also of the same form as Eq. (24) above. The value of γ may be different in both cases. The selection rule, associated with (A19), for the allowed values of L will be

$$\mathbf{J}(f) = \mathbf{J}(i) + \mathbf{L} + \tfrac{1}{2},$$

instead of Eq. (25) above.

PHYSICAL REVIEW VOLUME 120, NUMBER 4 NOVEMBER 15, 1960

Angular Distributions of the $Be^9(d,n)B^{10}$ Neutrons

RICHARD BARDES AND GEORGE E. OWEN
The Johns Hopkins University, Baltimore, Maryland
(Received July 7, 1960)

The angular distributions of neutrons to the ground state and to the first excited state of B^{10} in the reaction $Be^9(d,n)B^{10}$ have been studied at incident deuteron energies of 1.41 Mev, 1.88 Mev, and 2.35 Mev. A proton recoil spectrometer utilizing a xenon gas scintillation trigger was developed to study this problem. This spectrometer operated with a resolution of the order of 7% at the neutron energies involved in this reaction.

The analysis of the data in terms of a direct interaction mechanism indicates that the results are consistent with an interpretation which indicates that the majority of the neutrons emitted at bombarding energies below the Coulomb barrier originate in the Be^9 target nucleus.

I. INTRODUCTION

WHEN considering the general physical problem of nuclear stripping, the Be^9 nucleus is unique. Deuteron stripping has in general been thought of as a consequence of the low binding energy of the proton relative to the neutron; a low binding energy implying an extended wave function and thus a large average separation of the nucleons.

The Be^9 nucleus not only has a lower binding energy for the last neutron, but in addition this particular neutron is in a P state. Thus the average separation of the last neutron from the Be^9 core is even greater than the average extension of the deuteron. Thus one[1] should expect that the outer neutron would be stripped off quite readily.

In spite of the fact that the reaction is of fundamental interest, only a limited number of experiments[2,3] have been performed to study these neutrons. The major experimental difficulty has been that the $Be^9(d,n)B^{10}$ reaction results in neutron groups of relatively low energy and groups which are relatively close in energy. When one considers this fact along with the presence of a high background of gamma rays, it is apparent that high-resolution neutron spectroscopy associated with low background rates is required.

The previous work[2,3] was done utilizing photographic plate techniques, and in one case a time-of-flight method was used to measure the first excited state group.[3] This earlier work performed at low energies indicated the possibility of stripping from the Be^9 nucleus.

The results to be reported here were extended to higher energies with better statistics. In addition to the angular distributions, the total cross sections for the ground and first excited state transitions were measured. The detector used was a recoil proton telescope employing a gas scintillator as the trigger. This instrument will be described.

II. EXPERIMENTAL ARRANGEMENT

The neutron spectrometer used in these experiments was of the same type as developed by other experimenters,[4] with the exception of the trigger mechanism. The conventional telescope employs a trigger which

[1] G. E. Owen and L. Madansky, Phys. Rev. **99**, 1608 (1955).
[2] F. Ajzenberg, Phys. Rev. **88**, 298 (1952); J. S. Pruitt, C. D. Swartz, and S. S. Hanna, Phys. Rev. **92**, 1456 (1953); L. L. Green, J. P. Scanlon, and J. C. Willmott, Proc. Phys. Soc. (London) **A68**, 386 (1955); A. I. Shpetny, J. Exptl. Theoret. Phys. (U.S.S.R.) **32**, 423 (1957) [translation: Soviet Phys. JETP **5**, 357 (1957)].
[3] G. C. Neilson, J. T. Sample, and J. B. Warren, *Fast Neutron Physics* (Interscience Publishers, New York, to be published).
[4] C. H. Johnson, *Fast Neutrons Physics* (Interscience Publishers, New York, to be published), Chap. IIC.

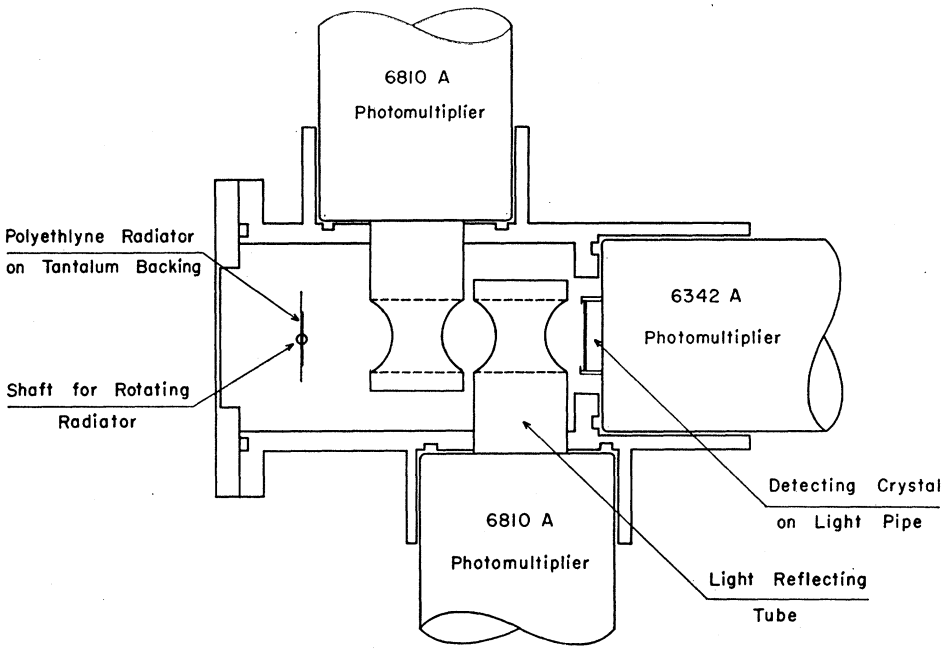

FIG. 1. Diagram of the gas scintillation proton recoil telescope.

requires the proton recoils to pass through two proportional counters that are between the radiator and the detector. Signals from these counters are used to operate a slow coincidence circuit whose output gates a multichannel pulse-height analyzer on which signals from the detector are displayed. The use of proportional counters as discriminators has several undesirable features. The response times are different for protons passing at different distances from the center wire, and also, the sensitive volume of the trigger is large, which enhances the accidental rate.

In this experiment, the proportional counters were replaced by photomultiplier tubes that detected the scintillations produced in xenon during the passage of the recoil protons.[5–7]

Figure 1 is a cross-section view of the counting chamber which was bored from a brass block. The reflecting tubes were constructed from thin-walled aluminum tubing and were closed off with a mirror made by evaporating a thin coating of aluminum on a microscope slide cover. The reflecting surfaces as well as the photomultiplier tube faces were coated with a thin transparent layer of about 80 $\mu g/cm^2$ of quater phenyl which acted as a wavelength shifter, since the rare gas scintillations are mainly in the ultraviolet.

Aside from their use as reflectors, these tubes served to reduce and isolate the volume of gas to which each photomultiplier tube is sensitive.

Since rare gas scintillations are very susceptible to the poisoning effects of contaminants, it was essential to use a continuously operating gas purification system. The system used was very similar to that employed by Wu and Sayres in which the gas is purified by passing it over hot calcium metal turnings. Figure 2 is a block diagram of the system used including the freeze-out tube for recovering the xenon.

The hydrogenous radiator consisted of a circle of polyethelene nominally one mil thick and having a $\frac{5}{8}$-inch diameter. It was mounted on a thin tantalum sheet by gentle heating so that it defines its own area.[8] The tantalum sheet is connected to a shaft that can be rotated externally. In this way the tantalum may be brought between the polyethylene and the detecting crystal, and the background determined. The mass-to-area ratio of the particular radiator used was found to be 2.22 ± 0.11 mg/cm^2.

The detector was a $\frac{3}{4}$-inch by a 20-mil CsI(Th) crystal mounted on a small glass light pipe. This in turn was coupled to an RCA 6342A photomultiplier tube using silicone oil as the optical coupling. A tantalum exit aperture having a $\frac{5}{8}$-inch diameter was mounted just in front of the crystal and thus defined the beam diameter.

In Fig. 3 a block diagram is shown of the electronics. RCA 6810A photomultiplier tubes were employed to detect the rare gas scintillations. The tube bases were of standard design but had a large anode resistance in order to stretch the pulses to about 7 μsec. The outputs from the tube bases were fed into Hamner N-301 amplifiers that have integral pulse-height discriminators. The output from the latter are then used to trigger the coincidence circuit. Essentially, this circuit is that of Fisher and Marshall,[9] although for this experiment it was used as a slow coincidence circuit with a resolution of about

[5] A. Sayres and C. S. Wu, Rev. Sci. Instr. **28**, 758 (1957).
[6] R. A. Nobles, Rev. Sci. Instr. **27**, 280 (1956).
[7] J. A. Northrop and R. A. Nobles, Nucleonics **14**, 36 (1956).
[8] A. Galonsky and C. H. Judish, Phys. Rev. **100**, 121 (1955).
[9] J. Fisher and J. Marshall, Rev. Sci. Instr. **23**, 417 (1952).

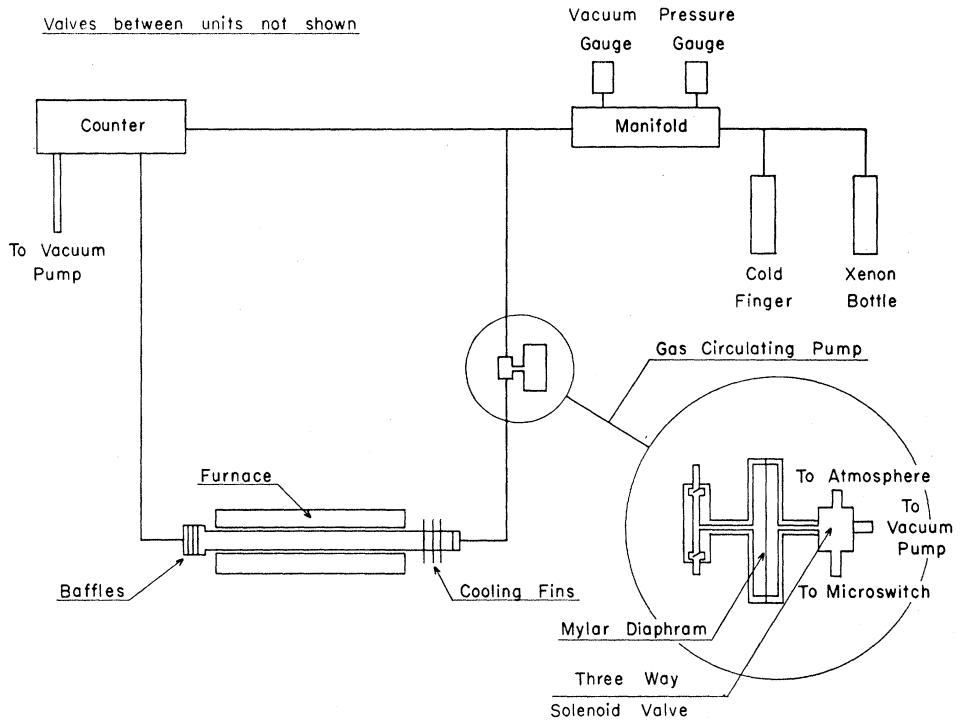

FIG. 2. Schematic diagram of the xenon gas handling system.

2 μsec. The coincidence pulse triggers a multivibrator which in turn gates a 100-channel pulse-height analyzer.

The efficiency of the telescope can be calculated from the radiator composition, radiator thickness, and the over-all geometry. Corrections must be made for the efficiency of the coincidence circuitry and for counting losses encountered because of dead time in the electronics. The geometric corrections of Bame *et al.*[10] were also applied.

The gas scintillation circuitry was tested for efficiency by allowing protons from the reaction $B^{10}(d,p)B^{11}$ to pass through a thin foil covering a hole in the face of the counter. The counting rate was then determined with and without the coincidence circuit in operation. With the Xenon pressure adjusted so that the protons lost about 600 kev in the gas, the efficiency was found to be 96.4%. This energy loss corresponds to that used in the actual experiment. Further tests were conducted in which the gas pressure was held constant and the discriminator settings varied, and also in which the discriminators were held constant and the gas pressure varied. These tests showed that moderate changes in either the gas pressure of discriminator settings produced no appreciable change in the coincidence circuit efficiency.

Counting losses arising from dead time in the electronics have been estimated and indicate further correction of about two percent.

Consideration has been given to other possible losses in efficiency such as attenuation and inscattering by the front face of the counter and multiple scattering by the gas and apertures. In both cases estimates of these effects were found to be negligible.

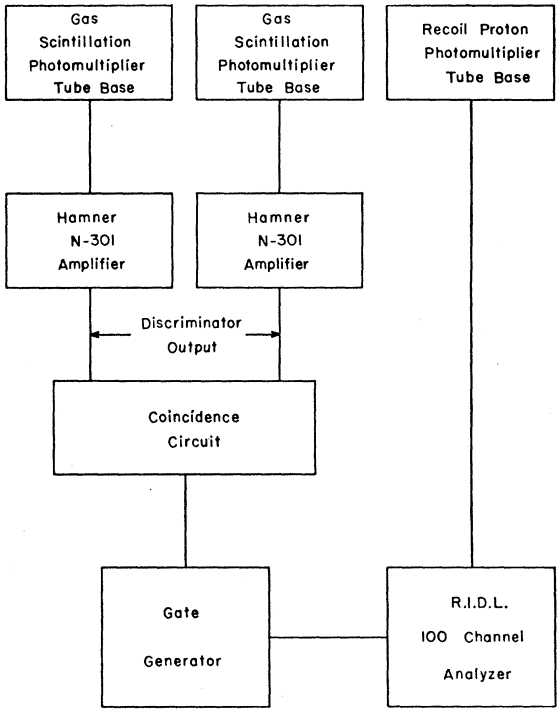

FIG. 3. Block diagram of the electronic arrangement.

[10] S. J. Bame, Jr., E. Haddad, J. E. Perry, Jr., and R. K. Smith, Rev. Sci. Instr. 28, 997 (1957).

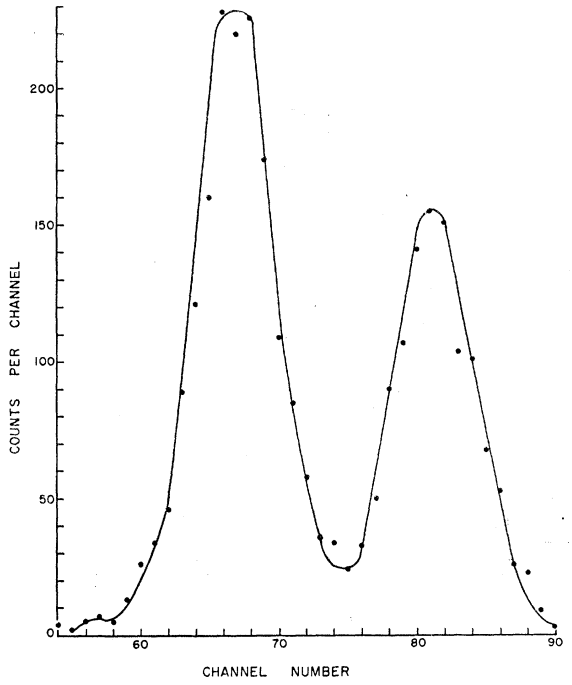

FIG. 4. Pulse-height spectrum of the proton recoils corresponding to transitions to the ground state and first excited state of B^{10}. These data were taken at a deuteron bombarding energy of 1.88 Mev with the counter at 90° relative to the beam axis.

The Be^9 targets were made by evaporating high-purity beryllium onto a five-mil copper backing. Their thickness was determined using the method of Fowler *et al.*[11] A further check is obtained by measuring the full width at half maximum of the thin target yield curve of the resonance in the reaction $Be^9(p,\gamma)B^{10}$. The average value obtained by these methods was 0.171 ± 0.035 mg/cm^2.

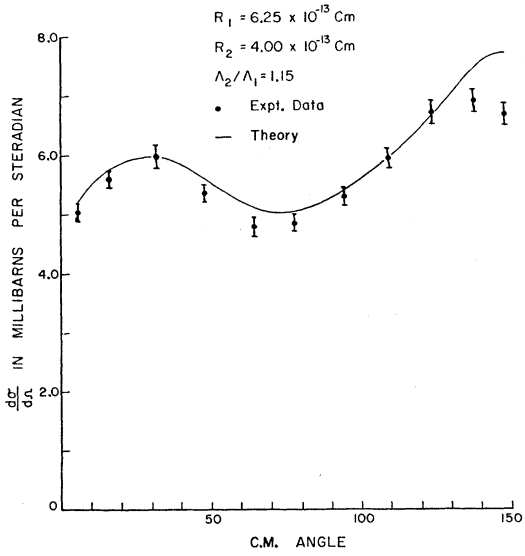

FIG. 5. Ground-state angular distribution at $E_d=1.41$ Mev.

[11] W. A. Fowler, C. Lauritsen, and T. Lauritsen, Revs. Modern Phys. **20**, 236 (1948).

III. EXPERIMENTAL PROCEDURE

The deuterons used in this experiment to obtain the angular distributions and yield curves were obtained from the Johns Hopkins University 3-Mev Van de Graff accelerator. The accelerator was calibrated by observing the resonance yield of 6–7 Mev gamma rays from the reaction $F^{19}(p,\alpha\gamma)O^{16}$ using fluorine targets made by evaporating a thin layer of ZnF on a copper backing.

Monitoring of the beam was accomplished using an Eldorado Electronics Company CI-100 current integrator. This instrument reads both the instantaneous beam current, which averaged about 10 microamperes, and the integrated beam current or total charge.

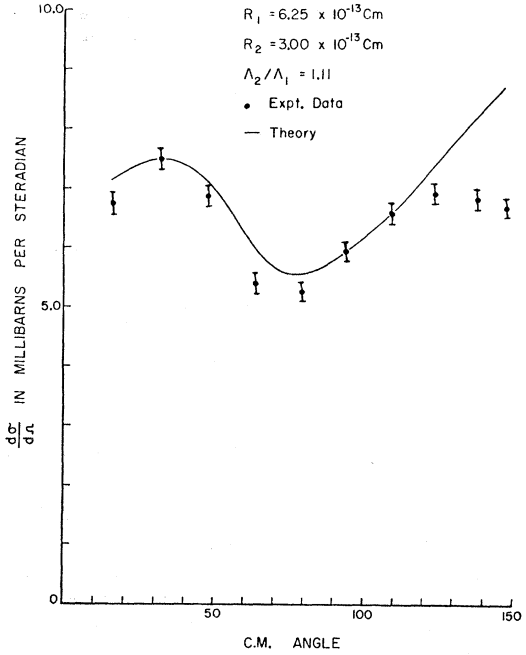

FIG. 6. Ground-state angular distribution at $E_d=1.88$ Mev.

After carefully positioning the counter at a given angle, Xenon at an average pressure of 320 mm of Hg was admitted to the counting chamber. In order to insure that the efficiency of the coincidence circuit would remain constant as the angle was varied, the gas pressure was reduced slightly as the counter was moved to larger angles. The variation in pressure was such that the average energy loss of the recoiling protons was constant.

On completing the count at a given angle, the radiator was rotated so that the tantalum backing was between the radiator and the detecting crystal. The deuterons were again permitted to strike the target, and in this way the background counting rate was determined. After completing the background count, the xenon was

frozen out and the system was evacuated to insure against the buildup of contaminants.

The same general procedure was used to obtain the yield curves, except that the angle remained fixed at 30° while the bombarding energy was varied.

In all cases rechecks were made at several of the angles or bombarding energies to insure that the results were consistent.

IV. EXPERIMENTAL RESULTS

The data were obtained in the form shown in Fig. 4. The two peaks corresponding to the ground-state and first excited state transitions are reasonably well separated; however, the final unfolding of the peaks was performed by using the tail of the line from the first excited state and the leading edge of the line from the ground-state transition to provide the over-all line shape.

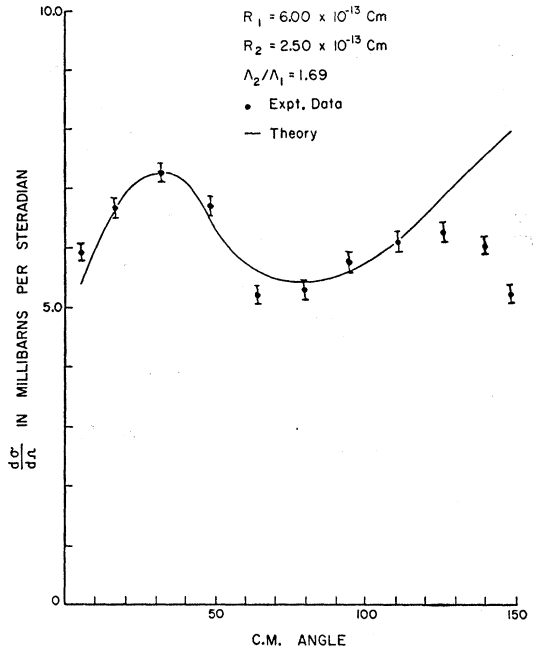

FIG. 7. Ground-state angular distribution at $E_d=2.35$ Mev.

The angular distributions are shown in Figs. 5–10. Table I gives the integrated total cross section, while Table II exhibits the yield curves for the neutrons emitted at 30° as a function of deuteron bombarding energy from 0.846 Mev to 2.35 Mev.

V. DISCUSSION AND ANALYSIS

The data were analyzed on the basis of a nuclear stripping formalism.[12] The forward peaks are consistent with an assignment of an orbital momentum capture of $l_p=1$. In the backward direction the fit utilizing a core capture angular momentum of $l_c=0$ is best at the lower bombarding energies. The tendency of the data to turn down at the larger angles, especially for the ground state at 1.88 and 2.35 Mev, can possibly arise from increased amounts of core capture angular momentum of $l_c=2$.

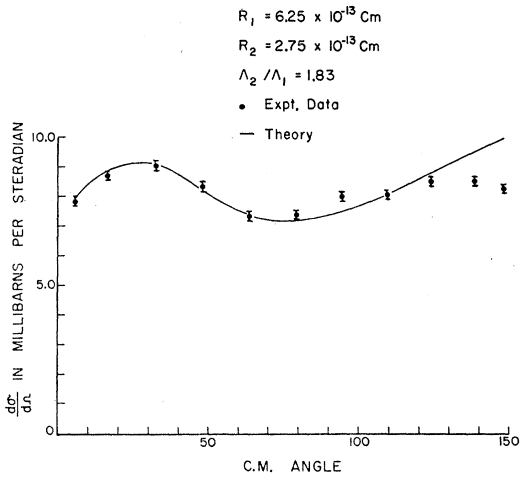

FIG. 8. First excited state angular distribution at $E_d=1.41$ Mev.

Using a j-j coupling scheme for the captured proton and deuteron in their respective modes, with the total angular momentum of B^{10} as 3, the final computed angular distribution for transitions to the ground state of B^{10} according to the theory of reference 12 is,

$$d\sigma/d\Omega \propto |\Lambda_1 C_1 G_D(K_1) F_D(k_1 R_1)|^2 - 0.669\Lambda_1\Lambda_2 C_1 C_2 G_D G_H F_D F_H \cos\beta + |\Lambda_2 C_2 G_H(K_2) F_H(k_2 R_2)|^2;$$

where β is the angle between $\mathbf{k}_1$ and $\mathbf{K}_2$, and $\mathbf{k}_j$. C_1, C_2, G_D, F_D, G_H, and F_H are defined in a previous paper.[12]

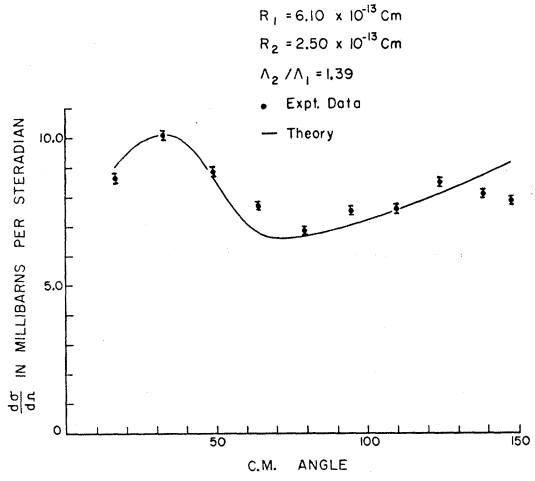

FIG. 9. First excited state angular distribution at $E_d=1.88$ Mev.

[12] G. E. Owen and L. Madansky, Phys. Rev. **105**, 1766 (1957); T. Fulton and G. E. Owen, Phys. Rev. **108**, 789 (1957); G. E. Owen, L. Madansky, and S. Edwards, Phys. Rev. **113**, 1575 (1959).

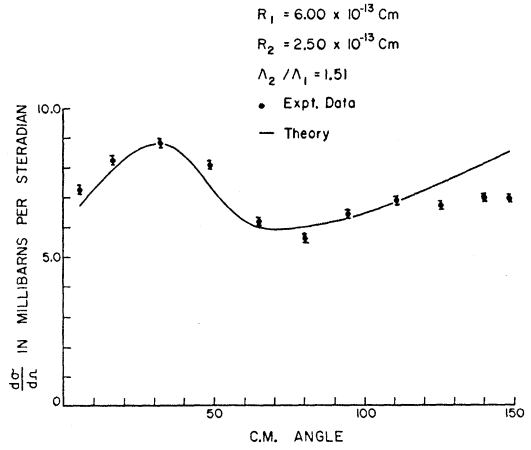

FIG. 10. First excited state angular distribution at $E_d=2.35$ Mev.

The differential cross section for transitions to the first excited state has a similar form with the exception that the interference term has a coefficient of -0.730 instead of -0.669 as in the case of the ground-state transition. In this case the total angular momentum of the excited B^{10} is taken as 1.

The use of $l_c=0$ rules out the Be^8 core having a spin of zero which may seem a little unsatisfactory. However, the generally accepted value of zero for the spin refers to a free Be^8 nucleus, and the assumption that the Be^9 spin of $\frac{3}{2}$ is formed from the simple coupling of the last $p_{\frac{3}{2}}$ neutron to a zero spin core is based on an extremely simplified version of the shell model that can neither predict the correct magnetic moment nor the correct energy levels. Also, pure J-J coupling is not believed to be completely accurate in the case of very light nuclei.

A more realistic picture of the Be^9 nucleus and also the final state B^{10} nucleus is obtained by using an intermediate coupled individual particle model in which the total spin and energy levels depend on all the nucleons. With such a model, it seems plausible that at the time of breakup, the core could have a spin of two.

The general trend of the angular distribution data seems to be an increasing ratio of the forward to backward component as the bombarding energy is increased. This is consistent with the results of other workers, in particular, Pruitt, Swartz, and Hanna,[2] who obtained angular distributions for the two states of interest at $E_d=0.945$ Mev having a large backward component, and Ajzenberg,[2] who obtained very pronounced forward peaks at 3.39 Mev, although these data go only to 80 degrees.

With respect to the yield curves, it is interesting to note that the dip at a bombarding energy slightly greater than one Mev occurs at about the same energy as a reported resonance in the $Be^9(d,d)Be^9$ elastic scattering cross section. This suggests that the "peak" in the (d,n) yield curve may not be a compound nucleus resonance at all but is simply the result of the (d,n) yield being depressed by the enhanced probability for elastic scattering.

The results indicate that the interpretation in terms of a two-mode direct interaction is a plausible one. The increase of the relative amount of deuteron stripping as the energy is increased is of course quite consistent with the picture of the Be^9 system as one which should exhibit stripping to the same or even greater extent than the deuteron. The analysis presented is based upon a Born approximation; therefore, no attempt should be made to consider the small details of the fits. At best the Born approximation can indicate that the direct-interaction picture is consistent with the experimental results. The final test of the validity of the analysis in terms of a direct interaction must arise from a more detailed distorted-wave calculation.

TABLE I. Total cross sections for the ground-state and first excited state transitions. These cross sections were obtained by numerical integration of the angular distributions.

E_d in Mev	σ in millibarns for ground state	σ in millibarns for first excited state
1.41	71±21	102±30
1.88	79±23	101±30
2.35	74±22	87±25

TABLE II. Yield as a function of deuteron bombarding energy. These data were obtained at a fixed angular setting of the counter. The angle between the counter and the beam axis was 30 degrees.

E_d in Mev	$d\sigma/d\Omega$ in millibarns/steradian for ground state	$d\sigma/d\Omega$ in millibarns/steradian for first excited state
0.846	3.70±0.16	4.05±0.15
0.940	5.48±0.19	5.86±0.18
1.04	2.31±0.12	4.64±0.16
1.13	2.71±0.13	6.44±0.19
1.32	5.94±0.19	9.65±0.23
1.50	7.73±0.22	11.02±0.25
1.69	8.69±0.23	11.10±0.26
1.88	8.75±0.24	10.23±0.25
2.35	8.26±0.23	10.23±0.24